Insulin-Like Growth Factor-I Promotes Neurogenesis and Synaptogenesis in the Hippocampal Dentate Gyrus during Postnatal Development

John R. O'Kusky,[1] Ping Ye,[2] and A. Joseph D'Ercole[2]

[1]*Department of Pathology and Laboratory Medicine, University of British Columbia, Vancouver, British Columbia, Canada V5Z 1M9, and* [2]*Department of Pediatrics, Division of Endocrinology, University of North Carolina at Chapel Hill, Chapel Hill, North Carolina 27599-7220*

The *in vivo* actions of insulin-like growth factor-I (IGF-I) on the growth and development of the hippocampal dentate gyrus were investigated in transgenic mice that overexpress IGF-I postnatally in the brain and in normal nontransgenic littermate controls. Stereological analyses of the dentate gyrus were performed by light and electron microscopy on days 7, 14, 21, 28, 35, and 130 to determine postnatal changes in the numerical density and total number of neurons and synapses. The volumes of both the granule cell layer and the molecular layer of the dentate gyrus were significantly increased by 27–69% in transgenic mice after day 7, with the greatest relative increases occurring by day 35. Although the numerical density of neurons in the granule cell layer did not differ significantly between transgenic and control mice at any age studied, the total number of neurons was significantly greater in transgenic mice by 29–61% beginning on day 14. The total number of synapses in the molecular layer was significantly increased by 42–105% in transgenic mice from day 14 to day 130. A transient increase in the synapse-to-neuron ratio was found in transgenic mice at postnatal days 28 and 35 but not at day 130. This finding indicates a disproportionate increase in synaptogenesis, exceeding that expected for the observed increase in neuron number. Our results demonstrate that IGF-I overexpression produces persistent increases in the total number of neurons and synapses in the dentate gyrus, indicating that IGF-I promotes both neurogenesis and synaptogenesis in the developing hippocampus *in vivo*.

Key words: insulin-like growth factor-I; IGF-I; hippocampus; dentate gyrus; neurogenesis; synaptogenesis; stereology

Insulin-like growth factor-I (IGF-I) is a 70 amino acid anabolic peptide that promotes growth and development of the CNS (D'Ercole et al., 1996; Folli et al., 1996). IGF-I and its cognate receptor, the type I IGF receptor, are expressed throughout the brain during early development. IGF-I mRNA reaches peak expression in rodents during the first 2 postnatal weeks (Bach et al., 1991; Bartlett et al., 1991), exhibiting a transient expression in specific brain regions corresponding to periods of axon outgrowth, dendritic maturation, and synaptogenesis (Bondy, 1991).

IGF-I stimulates the proliferation of neuron progenitors, induces the differentiation of oligodendrocytes, and increases the survival of neurons and oligodendrocytes *in vitro* (McMorris and Dubois-Dalcq, 1988; Torres-Aleman et al., 1990; Drago et al., 1991; Mozell et al., 1991; Barres et al., 1992; Pons and Torres-Aleman, 1992; D'Mello et al., 1993; Werther et al., 1993). In homozygous mice, disruption of either the IGF-I gene or the type I IGF receptor gene produces pathological abnormalities and brain growth retardation (Baker et al., 1993; Liu et al., 1993). Brain growth retardation also occurs in transgenic mice that ectopically express IGF binding protein-1 in the brain, likely because of an inhibition of IGF-stimulated growth (D'Ercole et al., 1994; Ni et al., 1997). In transgenic mice that overexpress IGF-I in brain, the size and weight of the brain increase markedly (Mathews et al., 1988) because of an apparent increase in neuron number (Behringer et al., 1990) and increases in both total brain myelin (Carson et al., 1993) and regional density of myelinated axons (Ye et al., 1995).

Received June 9, 2000; revised Aug. 25, 2000; accepted Aug. 30, 2000.

This study was supported by National Institutes of Health Grant HD08299 and Medical Research Council of Canada/Canadian Neurotrama Research Program Grant MOP 37536 (Rick Hansen Institute, NeuroScience Canada Foundation, NeuroPartners Canada, Ontario Neurotrama Foundation, Alberta Paraplegic Foundation, and British Columbia Neurotrama Initiative).

Correspondence should be addressed to John R. O'Kusky, Department of Pathology and Laboratory Medicine, Room 364, C-Floor, Heather Pavilion, 2733 Heather Street, Vancouver, British Columbia, Canada V5Z 1M9. E-mail: jrokusky@interchange.ubc.ca.

The present study was conducted to investigate the *in vivo* effects of IGF-I on neurogenesis and synaptogenesis in the hippocampal dentate gyrus, using a line of transgenic mice that overexpress IGF-I exclusively in the brain during postnatal development (Ye et al., 1996). Neurogenesis in the dentate gyrus of normal rodents occurs predominantly between embryonic day 14 and postnatal day 20 (Stanfield and Cowan, 1979; Bayer, 1980). New neurons, however, continue to be generated throughout life, originating from subgranular stem cells (Altman and Das, 1965; Kuhn et al., 1996). Synaptogenesis in the dentate gyrus of rodents is most active between postnatal days 7 and 30 (Crain et al., 1973; Steward and Falk, 1986). Expression of the transgene in these mice begins at approximately the time of birth, increases to peak levels at 20–30 d of age, and then remains constant throughout life, resulting in increased brain weight after day 10 with concomitant enlargement of the brainstem, cerebellum, diencephalon, hippocampus, and cerebral cortex (Ye et al., 1996; Dentremont et al., 1999). These transgenic mice, therefore, provide a unique opportunity to investigate the *in vivo* role of IGF-I in controlling the final number of neurons and synapses generated in the dentate gyrus during postnatal development. Stereological analyses were performed by light and electron microscopy to investigate postnatal changes in the numerical density and total number of neurons and synapses in transgenic mice and in their normal nontransgenic littermate controls.

MATERIALS AND METHODS

Transgenic animals. Detailed protocols for the production of transgenic mice with significantly increased expression of IGF-I in the brain and their normal littermate controls have been published previously (Dai et al., 1992; Ye et al., 1996). Briefly, these transgenic mice (termed IGF-II/IGF-I transgenics) carry a 6.9 kb fusion gene that uses a 5.7 kb fragment of the 5′ mouse IGF-II genomic regulatory region to drive the expression of a human IGF-I cDNA (Dai et al., 1992). These mice were backcrossed more than six generations using the C57BL/6 background strain. IGF-II/IGF-I transgenic mice were bred as heterozygotes, and their normal, nontransgenic littermates were used as controls. Transgenic mice were routinely identified by PCR of tail genomic DNA. Mice were housed in the Trans-

genic Mice Facility of the Program in Molecular Biology and Biotechnology (University of North Carolina at Chapel Hill), maintained at a temperature of 22°C with 12 hr light/dark cycles, and were provided access to water and a standard pelleted diet *ad libitum*. All procedures were approved by the institutional review committees of the University of North Carolina at Chapel Hill and the University of British Columbia.

Histology. Pairs of IGF-II/IGF-I transgenic mice and normal littermate controls, matched for age and sex, were studied on postnatal days 7, 14, 21, 28, 35, and 130. Three matched pairs were examined on each of days 7, 14, and 21, and four matched pairs were examined on each of days 28, 35, and 130. Individual mice were deeply anesthetized by an intraperitoneal injection of sodium pentobarbital (80 mg/kg) and perfused through the ascending aorta for 1 hr with a fixative solution containing 4% paraformaldehyde and 1% glutaraldehyde in 0.1 M phosphate buffer, pH 7.4. The brains were removed, weighed, and placed in the same fixative solution at 4°C for an additional 24–48 hr. The brainstem and cerebellum were removed by a transverse cut through the inferior colliculus, and the paired cerebral hemispheres were bisected in the midline. From the left hemisphere of each brain, serial frozen sections were cut at 30 μm in the frontal plane through the entire rostrocaudal length of the cerebral hemisphere. Every second section in this series was mounted on a glass slide and stained for Nissl substance using 0.1% thionine in acetate buffer, pH 3.7. From the right hemisphere of each brain, five to six serial blocks of tissue (0.5-mm-thick) were sampled for electron microscopy with the aid of a dissecting microscope through the entire rostrocaudal length of the hippocampus, including both the suprapyramidal and infrapyramidal blades of the hippocampal dentate gyrus. Tissue blocks were washed in 0.1 M phosphate buffer and post-fixed for 12 hr in 1% buffered osmium tetroxide. After washing in acetate buffer, the blocks were stained with 2% aqueous uranyl acetate for 1 hr, followed by dehydration in ascending grades of ethanol, equilibration in propylene oxide, and embedding in Epon (Jembed 812; Canemco, Montreal, Quebec, Canada). From the rostral surface of each block, 10–12 serial semithin (0.7 μm) sections were cut, mounted on glass slides, and stained with 1% toluidine blue in 0.4% sodium borate. Individual blocks were trimmed down to prepare sections spanning the entire width of both the molecular layer (ML) and granule cell layer (GCL) of the dentate gyrus along the suprapyramidal blade. After trimming each block, three to five serial ultrathin sections of silver-gray interference color were cut, individually mounted on Formvar-coated slot grids, and stained with lead citrate.

Stereology. The serial frozen sections stained with thionine were used to determine the total volumes of the ML and the GCL of the dentate gyrus, using Cavalieri's direct estimator (Gundersen et al., 1988a). Briefly, individual sections were visualized using an Olympus BH-2 compound microscope (10× planapochromatic objective) interfaced to a BIOQUANT TCW98 image analysis system (R&M Biometrics, Nashville, TN) and viewed on a video monitor at a final magnification of 188×. The areas occupied by the ML and GCL were measured on the full series of 40–50 sections for each animal in square millimeters, following the boundary criteria of Franklin and Paxinos (1997) for the mouse. The total volume of each layer was calculated from $V = \Sigma A \times T \times 2$, where ΣA is the sum of area measurements, T is the section thickness, and 2 is the periodicity of the section sample.

The serial Epon-embedded semithin sections stained with toluidine blue were used to determine the numerical density of neurons (N_V, neurons per cubic millimeter) in the GCL, using the physical disector method (Gundersen et al., 1988b). For each tissue block, the first and fifth serial sections were chosen as the reference and look-up sections, respectively. Individual reference sections were examined with a 10× planapochromatic objective, and the boundary of the GCL, including both the suprapyramidal and infrapyramidal blades, was traced. The BIOQUANT TCW98 Stereology Toolkit (R&M Biometrics) was used to generate a random set of 8–10 sampling coordinates for the GCL on each reference section. At each sampling point, sections were visualized using a 100× oil-immersion planapochromatic objective at a final magnification of 1880× on the video monitor. A square counting frame, measuring 80 μm on a side, was used to count the nuclei of neurons in the GCL. The counting frame was placed over the GCL at each sampling point on the reference section, and the outlines of neuronal nuclei were drawn if they were positioned within the counting frame or intersected by its inclusion edges (e.g., the top and right edges). The corresponding microscopic field on the look-up section was then visualized, and the tracings from the reference section were redrawn on the video monitor. Neurons were counted with the disector if their nuclear profile was observed on the reference section but not on the look-up section. For each brain, 24–30 disectors from four to five serial tissue blocks were used to count a total of 226–304 neurons per animal. The N_V of neurons in the GCL was calculated from $N_V = \Sigma Q^- / \Sigma V_{Dis}$, where ΣQ^- is the sum of the neurons counted and ΣV_{Dis} is the sum of the disector volumes. The disector volume was calculated from $V_{Dis} = a_{Dis} \times h$, where a_{Dis} is the area of the counting frame, and h is the disector height (i.e., the distance separating the paired sections). Section thickness was determined by re-embedding several semithin sections from each block in Epon and cutting ultrathin sections of silver-gray interference color at right angles to the original plane of section. These ultrathin sections were mounted on #200 square mesh grids, stained with lead citrate, and examined by electron microscopy at a final magnification of 60,400×. The mean section thickness for all animals was determined to be 0.636 μm, and the mean disector height was calculated to be 2.544 μm. The total number of neurons in the GCL was calculated from estimates of neuronal N_V and total volume of the GCL. Calculating total neuron number, using estimates of tissue volume obtained from serial frozen sections and estimates of neuronal N_V obtained from Epon-embedded sections, could conceivably introduce a biased estimate given differential tissue shrinkage produced by the two different methods. However, we have determined previously that both histological methods produce a mean linear shrinkage of ~14% (range of 13.1–15.0%). Any systematic bias in the estimates of total neuron number would be negligible.

The serial ultrathin sections stained with lead citrate were used to determine the N_V of synapses in the ML of the dentate gyrus, using the physical disector method (Gundersen et al., 1988b; Mayhew, 1996). Briefly, for each tissue block, consecutive ultrathin sections were selected as the reference and look-up sections. Individual sections were examined by electron microscopy (Philips EM300) and contained an unobstructed view of the full depth of the ML. The outer (OML), middle (MML), and inner (IML) molecular layers were identified on each section based on the total depth of the ML for that section divided into thirds. Electron micrographs were taken at an initial magnification of 3900× and enlarged photographically to a final magnification of 10,700×. On the reference sections, four to six micrographs were sampled randomly from each of the OML, MML, and IML over three to four serial blocks from each brain. In the four matched pairs of transgenic and control mice at day 28, 12–18 micrographs were randomly sampled from each of the OML, MML, and IML to calculate the N_V of synapses within individual sublaminae of the ML. A second series of electron micrographs was sampled from the equivalent ultrastructural fields on the look-up sections. Micrographs were examined with a dissecting microscope (variable magnification 6–10×) for a final magnification of 64,200–107,000×. At this magnification, all synaptic contacts could be identified unequivocally, and a relatively large number of synapses could be sampled. A calibration standard (carbon grating replica) was photographed and printed with each series of micrographs. A transparency containing a counting frame was superimposed on each electron micrograph from the reference section, with the edges of the counting frame recessed from the borders of the micrograph by an appropriate guard area. Synapses were identified by the presence of two or more synaptic vesicles in a presynaptic axon and the apposition of differentiated presynaptic and postsynaptic membranes. Synapses were counted if the synaptic profile was observed within the counting frame or intersected by its inclusion edges but was not observed on the look-up micrograph. For each brain, 12–18 disectors from three to four serial tissue blocks were used to count 234–301 synapses. The N_V of synapses in the ML was calculated from $N_V = \Sigma Q^- / \Sigma V_{Dis}$, as described above for neurons. The thickness of ultrathin sections was measured using Small's method of minimal folds (Weibel, 1979), with minimal folds being photographed at a magnification of 102,000×. The mean section thickness was found to be 0.058 μm. The total number of synapses in the ML was calculated from estimates of synaptic N_V and total volume of the ML. For the four matched pairs of mice at day 28, the N_V and total number of synapses was determined individually for the OML, MML, and IML.

Statistical analysis. For most variables, the statistical significance of differences among means was determined with a 2 × 6 (groups × ages) ANOVA. For estimates of the N_V of synapses in individual laminae of the ML on day 28, differences among means were analyzed with a 2 × 3 (groups × laminae) ANOVA. The statistical significance of differences between individual pairs of means was analyzed by the Student–Newman–Keuls method, with values of $p < 0.05$ considered statistically significant.

RESULTS

Postnatal changes in brain weight and body weight for IGF-II/IGF-I transgenic mice and normal controls are illustrated in Figure 1. Normal development was characterized by a rapid increase in brain weight between postnatal days 7 and 28, followed by a more gradual increase to day 130 (Fig. 1*A*). Brain growth in IGF-II/IGF-I transgenic mice was substantially increased. Although brain weight did not differ significantly between the two groups on day 7, significant increases were observed in transgenic mice on days 14 (16%), 21 (18%), 28 (24%), 35 (22%), and 130 (35%). Because transgene expression is restricted to the brain, body weight did not differ significantly between transgenic and control mice at any age (Fig. 1*B*).

Histological examination of the serial frozen sections stained for Nissl substance revealed no signs of gross malformation or pathological abnormalities in the transgenic mice. However, at most ages, there were subtle but apparent increases in the size of the cerebral cortex, cerebellum, and the major regions of the diencephalon and telencephalon, consistent with increased brain weight. After day 14, there was a marked increase in the size of the hippocampal dentate gyrus in transgenic mice, recognized on individual sections by a noticeable increase in the thickness of both the GCL and the

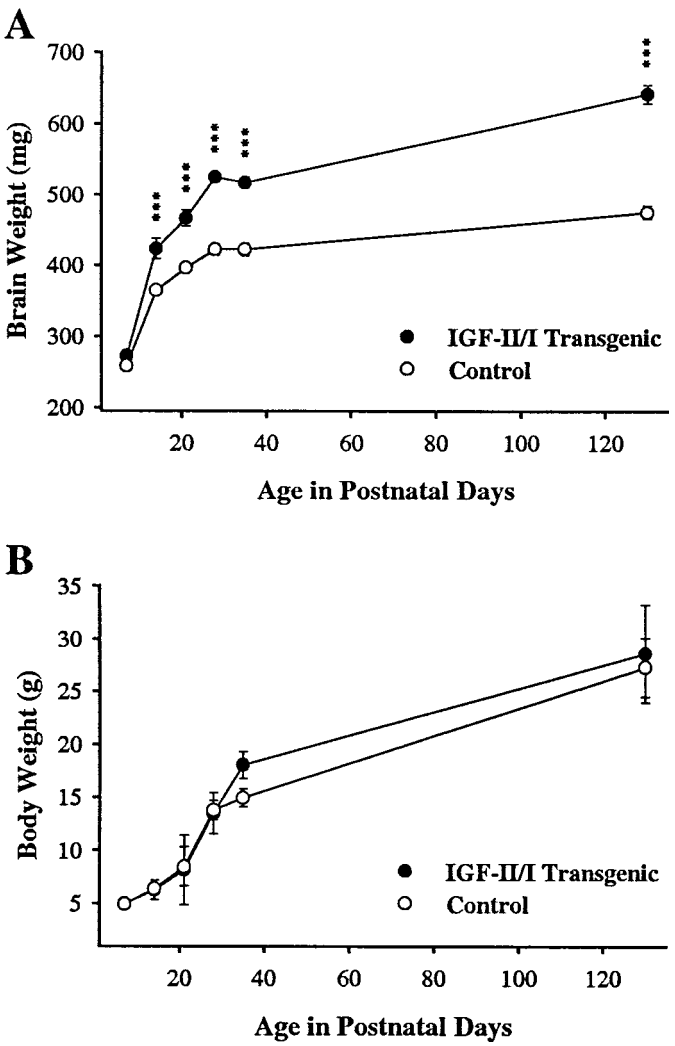

Figure 1. Postnatal changes in brain weight (*A*) and body weight (*B*) for IGF-II/IGF-I transgenic mice and normal littermate controls. Values are presented as the mean ± SEM for three to four mice in each group. ANOVA for brain weight revealed significant main effects for groups ($F = 277$; $p < 0.001$), ages ($F = 241$; $p < 0.001$), and group × age interactions ($F = 17.19$; $p < 0.001$). ***$p < 0.001$ for individual paired comparisons between transgenic and control mice. ANOVA for body weight revealed a significant main effect for age ($F = 120$; $p < 0.001$) but no significant main effects for groups ($F = 0.92$; $p = 0.35$) or group × age interactions ($F = 0.78$; $p = 0.57$).

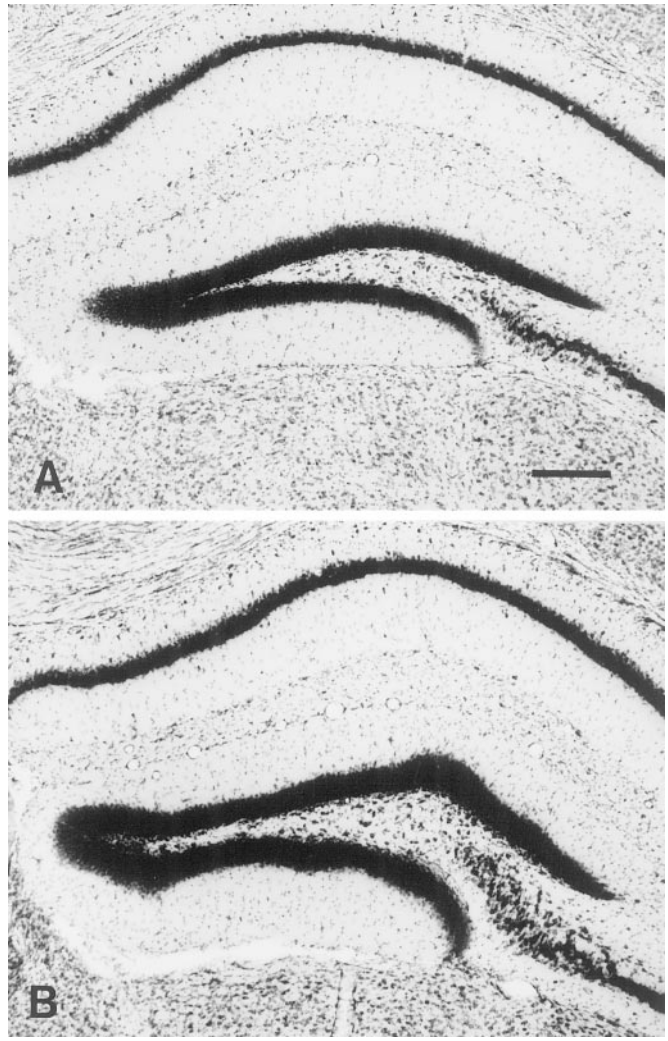

Figure 2. Representative sections of the hippocampal dentate gyrus in (*A*) normal control and (*B*) IGF-II/IGF-I transgenic mice at postnatal day 35. Serial frozen sections (30 μm) through the hippocampus were stained for Nissl substance with aqueous thionine. Scale bar, 250 μm.

ML (Fig. 2). A more subtle increase in the thickness of the pyramidal layer was observed in hippocampal regions CA1 to CA3 of transgenic mice, although an increased thickness of the molecular layer in these regions was not apparent (Fig. 2). Postnatal changes in the total volumes of the GCL and ML of the dentate gyrus in IGF-II/IGF-I transgenic mice and controls are illustrated in Figure 3. Normal development of the GCL in controls was characterized by a rapid increase in volume from day 7 to day 21, followed by a transient decrease at day 28. Control GCL volume increased between days 28 and 35, with no increase between days 35 and 130 (Fig. 3*A*). Although volume of the GCL did not differ significantly between the two groups on day 7, significant increases in volume were observed in transgenic mice on days 14 (45%), 21 (33%), 28 (59%), 35 (57%), and 130 (69%). As opposed to controls, the volume of the GCL in transgenic mice was observed to increase significantly (18%; $p < 0.01$) between days 35 and 130. The volume of the ML in controls increased from day 7 to day 21, remaining relatively constant to day 35, followed by a significant increase at day 130 (Fig. 3*B*). The volume of the ML in transgenic mice did not differ significantly from controls on day 7, but it was significantly greater on days 14 (38%), 21 (27%), 28 (51%), 35 (62%), and 130 (55%).

Postnatal changes in the total number of neurons in the GCL and the total number of synapses in the ML of IGF-II/IGF-I transgenic mice and controls are shown in Figure 4. In control mice, the total number of neurons in the GCL increased significantly from day 7 to day 35 (113%; $p < 0.001$), with no additional increase by day 130 (Fig. 4*A*). In transgenic mice, GCL neurons increased from day 7 to day 35 (172%; $p < 0.001$), with an additional significant increase between day 35 and day 130 (17%; $p < 0.01$). Compared with controls, the total number of GCL neurons in transgenic mice did not differ significantly on day 7, but significant increases were observed on days 14 (55%), 21 (29%), 28 (50%), 35 (56%), and 130 (61%).

Normal synaptogenesis in control mice (Fig. 4*B*) was characterized by a substantial increase in the total number of synapses in the ML from day 7 to day 35 (723%; $p < 0.001$), followed by a further significant increase from day 35 to day 130 (73%; $p < 0.001$). In transgenic mice, total synapses in the ML increased dramatically from day 7 to day 35 (1438%; $p < 0.001$) at approximately twice the rate observed in controls. Although there was an additional significant increase in synapses in transgenic mice from day 35 to day 130 (35%; $p < 0.001$), the magnitude of this increase was similar to that observed in controls (12.57×10^8 synapses for transgenics and 13.16×10^8 synapses for controls). Although the total number of

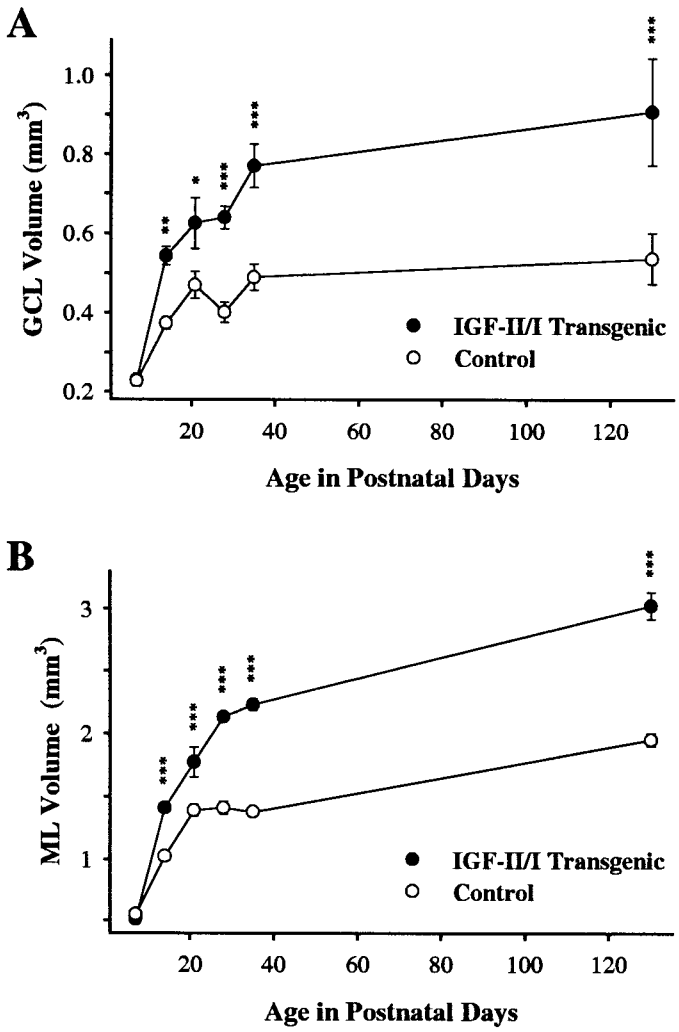

Figure 3. Postnatal changes in the total volumes of the GCL (*A*) and the ML (*B*) for IGF-II/IGF-I transgenic mice and normal littermate controls. Values are presented as the mean ± SEM for three to four mice in each group. ANOVA for volume of the GCL revealed significant main effects for groups ($F = 138$; $p < 0.001$), ages ($F = 60.86$; $p < 0.001$), and group × age interactions ($F = 8.59$; $p < 0.001$). ANOVA for volume of the ML revealed significant main effects for groups ($F = 275$; $p < 0.001$), ages ($F = 242$; $p < 0.001$), and group × age interactions ($F = 22.61$; $p < 0.001$). $^{*}p < 0.05$; $^{**}p < 0.01$; $^{***}p < 0.001$ for individual paired comparisons between transgenic and control mice.

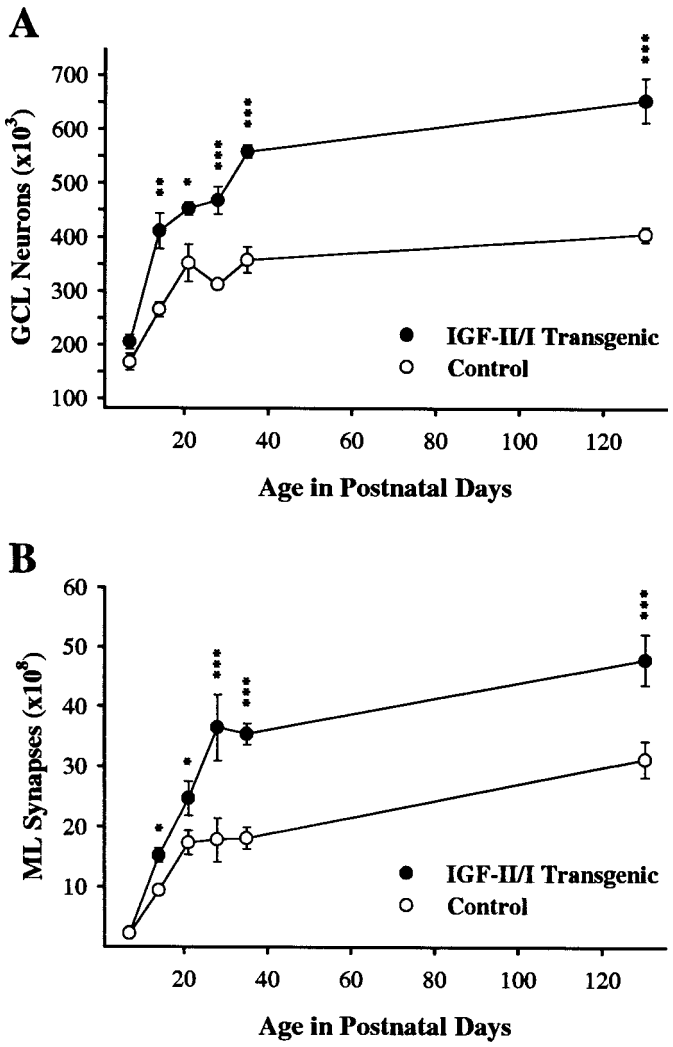

Figure 4. Postnatal changes in the total numbers of neurons in the GCL (*A*) and the total of synapses in the ML (*B*) for IGF-II/IGF-I transgenic mice and normal littermate controls. Values are presented as the mean ± SEM for three to four mice in each group. ANOVA for total neurons in the GCL revealed significant main effects for groups ($F = 118$; $p < 0.001$), ages ($F = 50.44$; $p < 0.001$), and group × age interactions ($F = 5.88$; $p < 0.001$). ANOVA for total synapses in the ML revealed significant main effects for groups ($F = 140$; $p < 0.001$), ages ($F = 131$; $p < 0.001$), and group × age interactions ($F = 11.25$; $p < 0.001$). $^{*}p < 0.05$; $^{**}p < 0.01$; $^{***}p < 0.001$ for individual paired comparisons between transgenic and control mice.

synapses in the ML did not differ significantly between transgenic and control mice on day 7 (Fig. 4*B*), significant increases were observed in transgenic mice on days 14 (61%), 21 (42%), 28 (105%), 35 (96%), and 130 (54%).

The N_V of neurons, expressed as the number of cells per cubic millimeter, did not differ significantly between transgenic and control mice at any stage of the experiment. Statistical analysis of neuronal N_V by ANOVA revealed no significant main effect for either groups ($F = 0.38$; $p = 0.54$) or ages ($F = 1.11$; $p = 0.38$), indicating that the packing density of GCL neurons did not change significantly during postnatal development. The mean N_V of GCL neurons ranged from $8.12 \pm 0.59 \times 10^5$ at day 7 to $7.43 \pm 0.26 \times 10^5$ at day 130. These results indicate that the significant increase in total neuron number in the GCL observed in transgenic mice was a function of increased tissue volume rather than a change in neuronal density.

As can be seen in Figure 5, neuronal packing density in the GCL of the dentate gyrus is inherently high. The granular neurons in the GCL are tightly packed with an almost juxtaposition of the cell soma, leaving a remarkably small volume of neuropil to separate the cells. The apical dendrites of these granular neurons ascend into the ML to receive the vast majority of synaptic contacts from afferent axons. Histological examination of the semithin sections stained with toluidine blue (Fig. 5) revealed no obvious differences in neuronal morphology between IGF-II/IGF-I transgenic and control mice.

Postnatal changes in the N_V of synapses in the ML of transgenic and control mice are illustrated in Figure 6*A*. Normal development in control mice was characterized by a rapid increase in the N_V of synapses from day 7 to day 35 (231%; $p < 0.001$), followed by a more gradual increase to day 130 (22%; $p < 0.05$). In transgenic mice, there was a 282% increase in the N_V of synapses from day 7 to day 28 ($p < 0.001$), with no significant changes observed after day 28. Compared with control mice, the N_V of synapses was significantly greater in transgenic mice on day 28 (36%; $p < 0.001$) and day 35 (21%; $p < 0.05$). When the N_V of synapses in individual sublaminae of the ML were compared at day 28 (Fig. 6*B*), increases in synaptic density were observed in transgenic mice in the OML (31%), MML (42%), and IML (36%). The ultrastructural appearance of synapses in the ML did not differ noticeably between transgenic and control mice. In older animals, the vast majority of

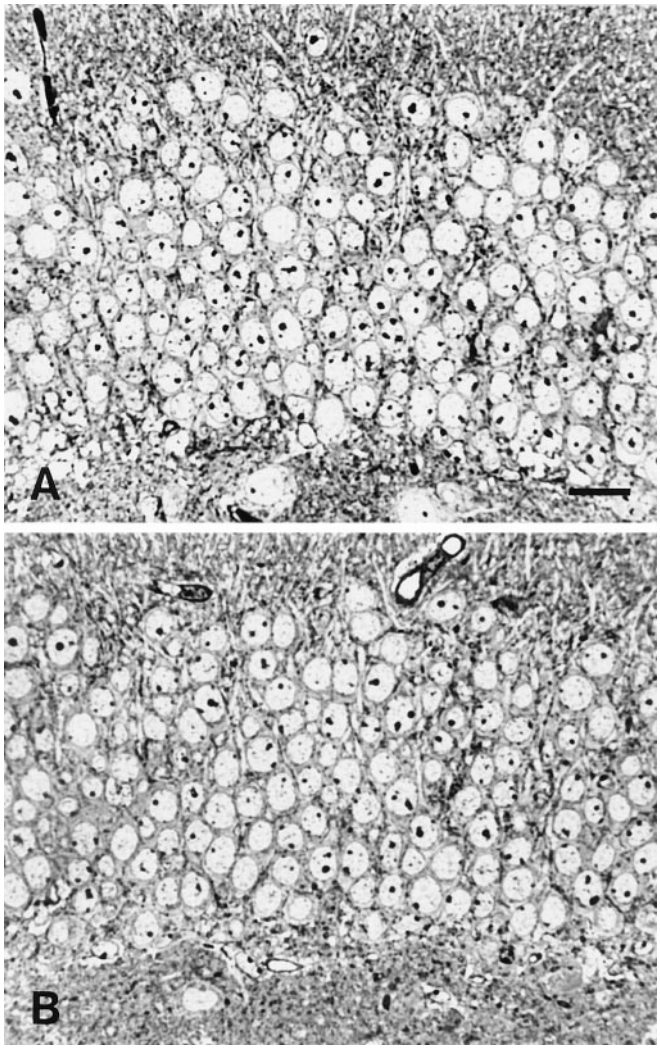

Figure 5. Epon-embedded semithin sections (0.7 μm) stained with toluidine blue through the GCL of the dentate gyrus in normal control (*A*) and IGF-II/IGF-I transgenic mice (*B*) at postnatal day 130. Scale bar, 20 μm.

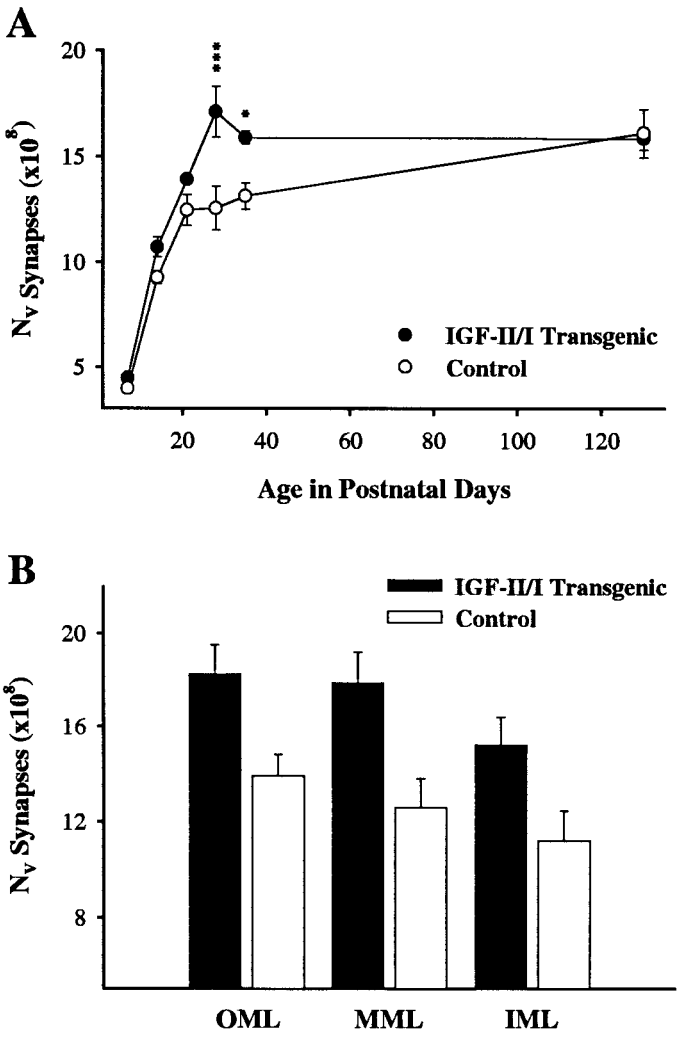

Figure 6. Postnatal changes in the N_V of synapses in the ML (*A*) for IGF-II/IGF-I transgenic mice and normal littermate controls. Values are presented as the mean ± SEM for three to four mice in each group. ANOVA for the N_V of synapses revealed significant main effects for groups ($F = 15.43$; $p < 0.001$), ages ($F = 62.55$; $p < 0.001$), and group × age interactions ($F = 2.82$; $p < 0.05$). $^*p < 0.05$; $^{***}p < 0.001$ for individual paired comparisons between transgenic and control mice. The N_V of synapses in the OML, MML, and IML (*B*) in transgenic and control mice on postnatal day 28. Values are given as the mean ± SEM for four mice in each group. ANOVA for the N_V of synapses in individual laminae revealed a significant main effect for group ($F = 21.58$; $p < 0.001$) but not for laminae ($F = 3.04$; $p = 0.07$) or group × laminae interactions ($F = 0.15$; $p = 0.86$).

synapses in the ML formed asymmetric axospinous contacts (Fig. 7*A*,*B*), although symmetric and asymmetric axodendritic synapses were occasionally observed (Fig. 7*C*). The mean length of synaptic contacts ranged from 0.19 to 0.23 μm in both transgenic and control mice across all ages studied. The only apparent qualitative difference between transgenic and control mice was in the diameter of dendritic profiles. In transgenic mice (Fig. 7*E*), the dendritic profiles appeared finer and more densely packed than in controls (Fig. 7*D*). This was most obvious in the OML and MML and more apparent on days 28 and 35 than at any other age. Given the rapid increase in volume of the ML at these ages, this observation suggests that the dendrites of granular neurons grow disproportionately in length rather than in girth. The significantly greater N_V of synapses in transgenic mice at these ages may result in part from a finer caliber of dendritic processes in the more superficial regions of the ML, which allows for a relatively greater packing density of synaptic contacts.

For each mouse, the synapse-to-neuron ratio in the dentate gyrus was calculated from estimates of the total number of neurons in the GCL and the total number of synapses in the ML (Fig. 8). Normal development was characterized by a rapid increase in the synapse-to-neuron ratio from day 7 to day 35 (283%; $p < 0.001$), followed by a more gradual increase to day 130 (51%; $p < 0.01$). In transgenic mice, this ratio increased from day 7 to a maximum value at day 28 (596%; $p < 0.001$) with no significant change occurring after day 28. Compared with controls, the synapse-to-neuron ratio in transgenic mice was significantly greater only on day 28 (60%; $p < 0.01$) and day 35 (24%; $p < 0.05$). At most ages, therefore, the increase in total ML synapse number in transgenic mice was attributable to an increase in the total number of neurons in the GCL, with each neuron being contacted by the normal complement of synapses. Only at days 28 and 35 were the synapse-to-neuron ratios significantly greater in transgenic mice, indicating that elevated expression of IGF-I augmented synaptogenesis over and above the increase in neuron number.

DISCUSSION

Our results demonstrate that IGF-I overexpression limited to the brain results in persistent increases in the total number of neurons and synapses in the dentate gyrus, indicating that IGF-I promotes both neurogenesis and synaptogenesis in the developing hippocampus *in vivo*. These findings are consistent with our previous studies of IGF-I transgenic mice showing that IGF-I stimulates both global and regional brain growth during early postnatal development (Mathews et al., 1988; Behringer et al., 1990; Ye et al., 1996;

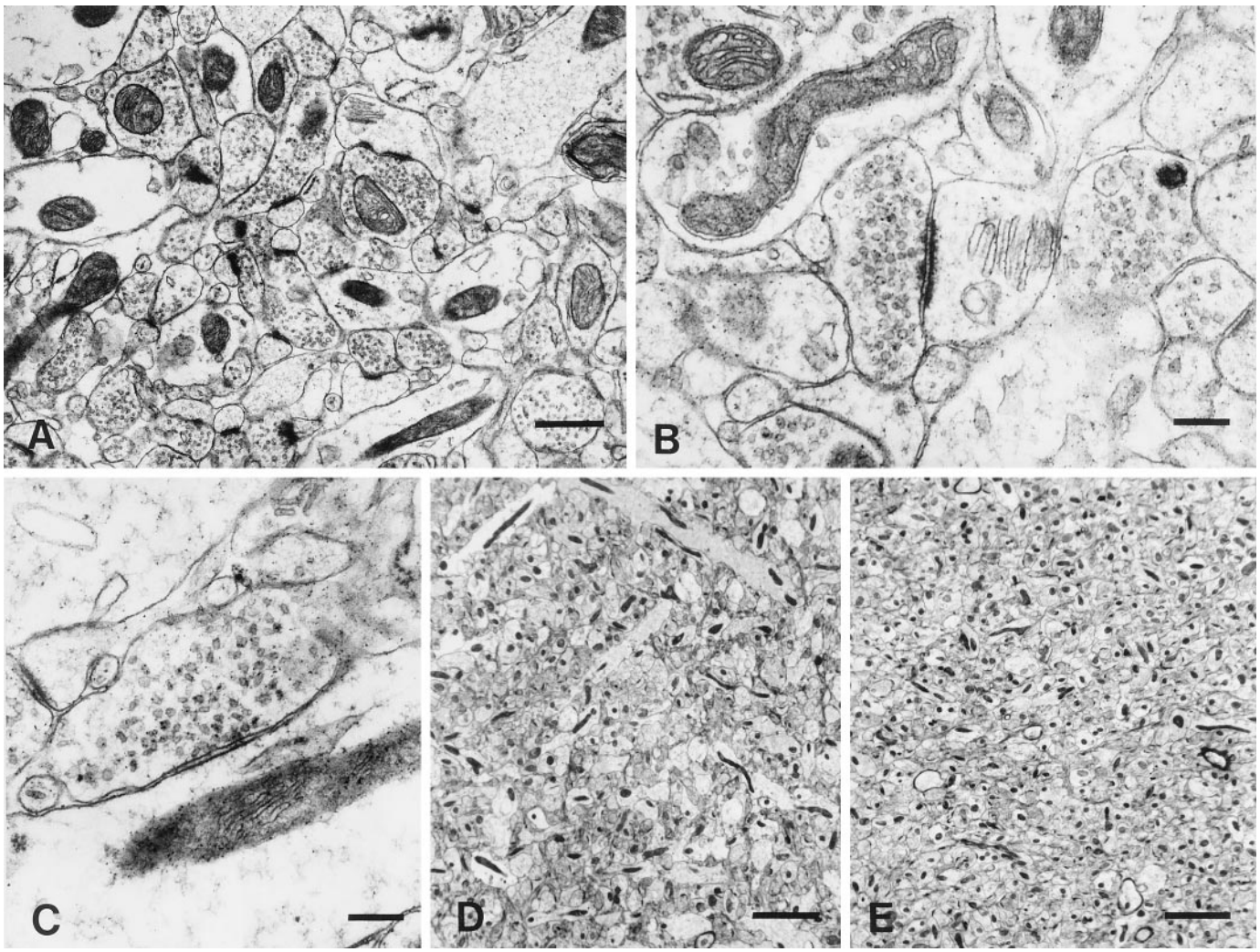

Figure 7. Electron micrographs from the ML of the dentate gyrus in IGF-II/IGF-I transgenic (*A–C*, *E*) and control (*D*) mice. The vast majority of synapses formed asymmetric axospinous contacts (*A*) in both transgenic and control mice, identified by the presence of a prominent postsynaptic density and predominantly spherical vesicles in the presynaptic axon terminal (*B*). Symmetric axodendritic contacts (*C*) were observed less frequently, identified by the presence of differentiated presynaptic and postsynaptic membranes without a prominent postsynaptic density and pleomorphic vesicles in the presynaptic axon terminal. Electron micrographs of the neuropil in the OML of normal control (*D*) and IGF-II/IGF-I transgenic (*E*) mice at postnatal day 28. Scale bars: *A*, 0.5 μm; *B*, *C*, 0.2 μm; *D*, *E*, 3 μm.

Dentremont et al., 1999). The accelerated brain growth in transgenic mice was not confounded by corresponding changes in somatic growth, because the body weights of the transgenic mice did not differ from those of their nontransgenic littermates because of the absence of transgene in tissues other than brain. The most rapid acceleration in neuron number occurred at a developmental stage when neuronal proliferation and apoptosis are active in the dentate gyrus, and IGF-I likely influenced both processes. The increased synapse-to-neuron ratios observed at days 28 and 35 indicate that IGF-I also stimulates synaptogenesis.

In IGF-II/IGF-I transgenic mice, there was an increase of 29–61% in the total number of neurons in the GCL, beginning at postnatal day 14 and persisting into young adult mice at day 130. This finding is consistent with previous studies showing decreased numbers of neurons in the dentate gyrus of IGF-I knock-out mice (Beck et al., 1995) and increased numbers of neurons in the brainstem and cerebellum of IGF-II/IGF-I transgenic mice (Ye et al., 1996; Dentremont et al., 1999). Among various inbred strains of mice, total neuron number in the GCL of the dentate gyrus can vary by as much as 50% (Wimer et al., 1988). Our estimate of the N_V of neurons in adult control mice at day 130 (743,000 neurons/mm^3) compares favorably with estimates of 640,000–800,000 neurons/mm^3 in adult rat (Curcio and Hinds, 1983). Similarly, our estimate of the total number of neurons in the GCL of adult

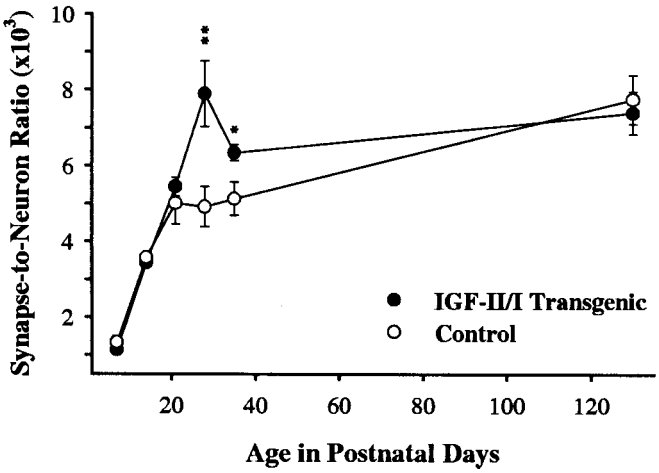

Figure 8. Postnatal changes in the synapse-to-neuron ratio in IGF-II/IGF-I transgenic mice and normal controls. Values are given as the mean ± SEM for three to four mice in each group. ANOVA revealed significant main effects for groups ($F = 4.88$; $p < 0.05$), ages ($F = 38.31$; $p < 0.001$), and group × age interactions ($F = 3.47$; $p < 0.05$). *$p < 0.05$; **$p < 0.01$ for individual paired comparisons between transgenic and control mice.

controls (~406,000) falls within the range of 300,000–640,000 reported by various authors for adult mice (Wimer et al., 1988; Demyanenko et al., 1999; Phinney et al., 1999).

During normal development, the final number of neurons to reach maturity in a given region of the brain is determined by the combined effects of neuron proliferation and naturally occurring neuron death. In the dentate gyrus of rats and mice, the proliferation of GCL neurons occurs predominantly from embryonic day 10 to postnatal day 20 (Angevine, 1965; Caviness, 1973; Stanfield and Cowan, 1979; Bayer, 1980). Progenitors of GCL neurons originate from the ventricular layer of the neural tube for a relatively short period of development before migrating into the dentate gyrus after embryonic day 14, at which peak proliferation continues until postnatal day 20. New neurons continue to be generated in the dentate gyrus at a reduced rate throughout adult life by subgranular stem cells with multilineage potential (Altman and Das, 1965; Kuhn et al., 1996). Unlike most regions of the brain, which have distinct periods of neuron proliferation and apoptotic cell death, the population of neurons in the GCL of the dentate gyrus exhibits substantial cell death during the time of peak neuron proliferation (Schlessinger et al., 1975; Wimer et al., 1988; Gould et al., 1991). In the dentate gyrus of rats, the density of pyknotic cells has been shown to peak at the end of the first postnatal week, although degenerating neurons have been observed as late as day 40 (Gould et al., 1991). Apoptotic neurons, detected in the dentate gyrus of mice by the terminal deoxynucleotidyl transferase-mediated biotinylated UTP nick end labeling method, are prominent from birth to day 21 (De Bilbao et al., 1999). Moreover, the expression of *cpp32* mRNA, which encodes for the caspase-3 cysteine protease and mediates apoptotic cell death, is maximal in the GCL during early postnatal development with continued expression in adults (De Bilbao et al., 1999). In several inbred strains of mice, the total number of GCL neurons decreases transiently during the fourth postnatal week (Wimer et al., 1988), reflecting the maximum rate of cell death before day 21.

The available evidence suggests that increased expression of IGF-I in these transgenic mice produces more neurons in the dentate gyrus by both increasing the rate of neuronal proliferation and decreasing the rate of cell death. IGF-I has been shown to promote the proliferation of neurons *in vitro* (DiCicco-Bloom and Black, 1988; McMorris and Dubois-Dalcq, 1988; Torres-Aleman et al., 1990; Drago et al., 1991; Werther et al., 1993; Zackenfels et al., 1995) and *in vivo* (Ye et al., 1996; Aberg et al., 2000). In contrast, IGF-I has well documented anti-apoptotic effects for cells in several tissues *in vitro* (Le Roith et al., 1997), and it has also been shown to promote neuron survival both *in vitro* and *in vivo* (Bozyczko-Coyne et al., 1993; Hughes et al., 1993; Neff et al., 1993; Mathews and Feldman, 1996; Dudek et al., 1998; Blair et al., 1999). In the present study, the normal transient decrease in neuron number between days 21 and 28 was not observed in transgenic mice, suggesting that elevated expression of IGF-I reduced apoptotic cell death. Similarly, neuron number continued to increase significantly after day 35 in transgenic mice but not in controls, suggesting that an IGF-I-mediated increase in the proliferation of GCL neurons continued throughout later stages of development into the young adult.

In IGF-II/IGF-I transgenic mice, there was a significant increase of 54–105% in the total number of synapses in the ML of the dentate gyrus, first noted at postnatal day 14 and persisting into the young adult. Furthermore, both the rate and time course of synaptogenesis differed substantially in transgenic and control mice. Our estimate of the N_V of synapses in the ML of the dentate gyrus in control mice at day 130 (16.11×10^8 synapses/mm^3) was 29% greater than estimates of N_V in the ML of adult rats (Curcio and Hinds, 1983) and 18% greater than estimates of N_V for the stratum radiatum of hippocampal CA1 in adult rabbits (Geinisman et al., 1996). In the present study, normal synaptogenesis in control mice was characterized by a relatively steady increase in both the N_V and total number of synapses throughout postnatal development into the young adult. In control mice, there was no evidence of synapse elimination during the later stages of postnatal development. Although synapse elimination in the dentate gyrus is not characteristic of rodents (Crain et al., 1973; Steward and Falk, 1986), it has been reported in the monkey (Eckenhoff and Rakic, 1991). Either the lack of a distinct period of synapse elimination in the dentate gyrus of rodents reflects substantial circuit formation at later stages of development by newly generated neurons, or synapse elimination may occur with peak synaptic densities being achieved after day 35.

The N_V of synapses in IGF-II/IGF-I transgenic mice increased rapidly from day 7 to day 28, with no additional increase in older mice. The synapse-to-neuron ratio was significantly greater in transgenic mice than in controls on days 28 and 35 but not in young adults, indicating an increase in synapse number over and above the observed increase in neuron number. These results are consistent with an initial augmentation of synaptogenesis during early postnatal development, followed by an apparent inhibition of further synapse formation after day 35. IGF-I is known to promote myelination of axons by stimulating gene expression for myelin-specific proteins and by promoting oligodendrocyte proliferation and survival (McMorris and Dubois-Dalcq, 1988; Mozell and McMorris, 1991; Ye et al., 1995). Reduced synaptogenesis in older transgenic mice could be explained by an increased production of one or more inhibitory factors (e.g., Nogo-A, the myelin-associated glycoprotein MAG, and the chondroitin sulfate proteoglycans versican V2 and brevican) by oligodendrocytes during myelination (Schwab and Caroni, 1988; Bandtlow and Schwab, 2000; Chen et al., 2000), which occurs predominantly after day 30 in mice for most brain regions.

Our findings demonstrate that IGF-I promotes growth and development of the hippocampal dentate gyrus by augmenting both neurogenesis and synaptogenesis during postnatal development. Although IGF-I promotes synaptogenesis in the early stages of postnatal development, it appears to be self-regulating, possibly by mechanisms involving increased myelination and the subsequent increased expression of factors inhibiting synaptogenesis at later stages.

REFERENCES

Aberg MAI, Aberg ND, Hedbacker H, Oscarsson J, Eriksson PS (2000) Peripheral infusion of IGF-I selectively induces neurogenesis in the adult rat hippocampus. J Neurosci 20:2896–2903.

Altman J, Das GD (1965) Autoradiographic and histological evidence of postnatal hippocampal neurogenesis in rats. J Comp Neurol 124:319–336.

Angevine JB (1965) Time of neuron origin in the hippocampal region: an autoradiographic study in the mouse. Exp Neurol [Suppl] 2:1–70.

Bach MA, Shen-Orr Z, Lower WL, Roberts CT, LeRoith D (1991) Insulin-like growth factor I mRNA levels are developmentally regulated in specific regions of the rat brain. Mol Brain Res 10:43–48.

Baker J, Liu J, Robertson EJ, Efstratiadis A (1993) Role of insulin-like growth factors in embryonic and postnatal growth. Cell 75:73–82.

Bandtlow CE, Schwab ME (2000) NI-35/250/Nogo-A: a neurite growth inhibitor restricting structural plasticity regeneration of nerve fibers in the adult vertebrate CNS. Glia 29:175–181.

Barres BA, Hart IK, Coles HS, Burne JF, Voyvodic JT, Richardson WD, Raff MC (1992) Cell death and control of cell survival in the oligodendrocyte lineage. Cell 70:31–46.

Bartlett WP, Li XS, Williams M, Benkovic S (1991) Localization of insulin-like growth factor-1 mRNA in murine central nervous system during postnatal development. Dev Biol 147:239–250.

Bayer SA (1980) Development of the hippocampal region in the rat. I. Neurogenesis examined with ^{3}H-thymidine autoradiography. J Comp Neurol 190:87–114.

Beck KD, Powell-Braxton L, Widmer HR, Valverde J, Hefti F (1995) IGF-I gene disruption results in reduced brain size, CNS hypomyelination, and loss of hippocampal granule and striatal parvalbumin-containing neurons. Neuron 14:717–730.

Behringer RR, Lewin TM, Quaife CJ, Palmiter RD, Brinster RL, D'Ercole AJ (1990) Expression of insulin-like growth factor I stimulates normal somatic growth in growth hormone-deficient transgenic mice. Endocrinology 127:1033–1040.

Blair LAC, Bence Hanulec KK, Mehta S, Franke T, Kaplan D, Marshall J (1999) Akt-dependent potentiation of L channels by insulin-like growth factor-I is required for neuronal survival. J Neurosci 19:1940–1951.

Bondy C (1991) Transient IGF-I gene expression during maturation of functionally related central projection neurons. J Neurosci 11:3442–3455.

Bozyczko-Coyne D, Glicksman MA, Prantner JE, McKenna B, Connors T,

Friedman C, Dasgupta M, Neff T (1993) IGF-I supports the survival and/or differentiation of multiple types of central nervous system neurons. Ann NY Acad Sci 692:311–313.
Carson MJ, Behringer RR, Brinster RL, McMorris FA (1993) Insulin-like growth factor I increases brain growth and central nervous system myelination in transgenic mice. Neuron 10:729–740.
Caviness Jr VS (1973) Time of neuron origin in the hippocampus and dentate gyrus of normal and reeler mutant mice: an autoradiographic analysis. J Comp Neurol 151:113–120.
Chen MS, Huber AB, van der Haar ME, Frank M, Schnell L, Spillmann AA, Christ F, Schwab ME (2000) Nogo-A is a myelin-associated neurite outgrowth inhibitor an antigen for monoclonal antibody IN-1. Nature 403:434–439.
Crain B, Cotman C, Taylor D, Lynch G (1973) A quantitative electron microscopic study of synaptogenesis in the dentate gyrus of the rat. Brain Res 63:195–204.
Curcio CA, Hinds JW (1983) Stability of synaptic density and spine volume in dentate gyrus of aged rats. Neurobiol Aging 4:77–87.
Dai Z, Takahashi SI, van Wyck JJ, D'Ercole AJ (1992) Creation of an autocrine model of insulin-like growth factor-I action in transfected FRTL-5 cells. Endocrinology 130:3175–3183.
De Bilbao F, Guarin E, Nef P, Vallet P, Giannakopoulos P, Dubois-Dauphin M (1999) Postnatal distribution of *cpp32*/caspase 3 mRNA in the mouse central nervous system: an *in situ* hybridization study. J Comp Neurol 409:339–357.
Demyanenko GP, Tsai AY, Maness PF (1999) Abnormalities in neuronal process extension, hippocampal development, and the ventricular system of L1 knockout mice. J Neurosci 19:4907–4920.
Dentremont KD, Ye P, D'Ercole AJ, O'Kusky JR (1999) Increased insulin-like growth factor-I (IGF-I) expression during early postnatal development differentially increases neuron number and growth in medullary nuclei of the mouse. Dev Brain Res 114:135–141.
D'Ercole AJ, Dai Z, Xing Y, Boney C, Wilke MB, Lauder JM, Han VK, Clemmons DR (1994) Brain growth retardation due to the expression of human insulin-like growth factor binding protein-1 (IGFBP-1) in transgenic mice: an *in vivo* model for the analysis of IGF function in the brain. Dev Brain Res 82:213–222.
D'Ercole AJ, Ye P, Calikoglu AS, Gutierrez-Ospina G (1996) The role of the insulin-like growth factors in the central nervous system. Mol Neurobiol 13:227–255.
DiCicco-Bloom E, Black IB (1988) Insulin growth factors regulate the mitotic cycle in cultured rat sympathetic neuroblasts. Proc Natl Acad Sci USA 85:4066–4070.
D'Mello SR, Galli C, Ciotti T, Calissano P (1993) Induction of apoptosis in cerebellar granule cells by low potassium: inhibition of death by insulin-like growth factor I and cAMP. Proc Natl Acad Sci USA 90:10989–10993.
Drago J, Murphy M, Carroll SM, Harvey RP, Bartlett PF (1991) Fibroblast growth factor-mediated proliferation of central nervous system precursors depends on endogenous production of insulin-like growth factor I. Proc Natl Acad Sci USA 88:2199–2203.
Dudek H, Datta SR, Franke TF, Birnbaum MJ, Yao R, Cooper GM, Segal RA, Kaplan DR, Greenberg ME (1998) Regulation of neuronal survival by the serine-threonine protein kinase Akt. Science 275:661–665.
Eckenhoff MF, Rakic P (1991) A quantitative analysis of synaptogenesis in the molecular layer of the dentate gyrus in the rhesus monkey. Dev Brain Res 64:129–135.
Folli F, Ghidella S, Bonfanti L, Kahn CR, Merighi A (1996) The early intracellular signalling pathway for the insulin/insulin-like growth factor receptor family in the mammalian central nervous system. Mol Neurobiol 13:155–183.
Franklin KBJ, Paxinos G (1997) The mouse brain in stereotaxic coordinates. San Diego: Academic.
Geinisman Y, Gundersen HJG, Van Der Zee E, West MJ (1996) Unbiased stereological estimation of the total number of synapses in a brain region. J Neurocytol 25:805–819.
Gould E, Woolley CS, McEwen BS (1991) Naturally occurring cell death in the developing dentate gyrus of the rat. J Comp Neurol 304:408–418.
Gundersen HJG, Bendtsen TF, Korbo L, Marcussen N, Moller A, Nielsen K, Nyengaard JR, Pakkenberg B, Sorensen FB, Vesterby A, West MJ (1988a) Some new, simple and efficient stereological methods and their use in pathological research and diagnosis. APMIS 96:379–394.
Gundersen HJG, Bagger P, Bendtsen TF, Evans SM, Korbo L, Marcussen N, Moller A, Nielsen K, Nyengaard JR, Pakkenberg B, Sorensen FB, Vesterby A, West MJ (1988b) The new stereological tools: disector, fractionator, nucleator and point sampled intercepts and their use in pathological research and diagnosis. APMIS 96:857–881.
Hughes RA, Sendtner M, Thoenen H (1993) Members of several gene families influence survival of rat motoneurons *in vitro* and *in vivo*. J Neurosci Res 36:663–671.
Kuhn HG, Dickinson-Anson H, Gage FH (1996) Neurogenesis in the dentate gyrus of the adult rat: age-related decrease of neuronal progenitor proliferation. J Neurosci 16:2027–2033.
Le Roith D, Parrizas M, Blakesley VA (1997) The insulin-like growth factor-I receptor and apoptosis- implications for the aging process. Endocrine 7:103–105.
Liu J, Baker J, Perkins AS, Robertson EJ, Efstratiadis A (1993) Mice carrying null mutations of the genes encoding insulin-like growth factor-I (IGF-1) and type-I IGF receptor. Cell 75:59–72.
Mathews CC, Feldman EL (1996) Insulin-like growth factor-I rescues SH-SY5Y human neuroblastoma cells from hyperosmotic induced programmed cell death. J Cell Physiol 166:323–331.
Mathews LS, Hammer RE, Behringer RR, D'Ercole AJ, Bell GI, Brinster RL, Palmiter RD (1988) Growth enhancement of transgenic mice expressing human insulin-like growth factor I. Endocrinology 123:2827–2833.
Mayhew TM (1996) How to count synapses unbiasedly and efficiently at the ultrastructural level: proposal for a standard sampling and counting protocol. J Neurocytol 25:793–804.
McMorris FA, Dubois-Dalcq M (1988) Insulin-like growth factor I promotes cell proliferation and oligodendroglial commitment in rat glial progenitor cells developing *in vitro*. J Neurosci Res 21:199–209.
Mozell RL, McMorris FA (1991) Insulin-like growth factor I stimulates oligodendrocyte development and myelination in rat brain aggregate cultures. J Neurosci Res 30:382–390.
Neff NT, Prevette D, Houenou JL, Lewis ME, Glicksman MA, Yin QW, Oppenheim RW (1993) Insulin-like growth factors: putative muscle-derived trophic agents that promote neuron survival. J Neurobiol 24:1578–1588.
Ni W, Rajkumar K, Nagy JI, Murphy LJ (1997) Impaired brain development and reduced astrocyte response to injury in transgenic mice expressing IGF binding protein-1. Brain Res 769:97–107.
Phinney AL, Calhoun ME, Wolfer DP, Lipp HP, Zheng H, Jucker M (1999) No hippocampal neuron or synaptic bouton loss in learning-impaired aged β-amyloid precursor protein-null mice. Neuroscience 90:1207–1216.
Pons S, Torres-Aleman I (1992) Basic fibroblast growth factor modulates insulin-like growth factor-I, its receptor, and its binding proteins in hypothalamic cell cultures. Endocrinology 131:2271–2278.
Schlessinger AR, Cowan WM, Gottlieb EI (1975) An autoradiographic study of the time of origin and the pattern of granule cell migration in the dentate gyrus of the rat. J Comp Neurol 159:149–176.
Schwab ME, Caroni P (1988) Oligodendrocytes and CNS myelin are non-permissive substrates for neurite outgrowth and fibroblast spreading *in vitro*. J Neurosci 8:2381–2393.
Stanfield BB, Cowan WM (1979) The morphology of the hippocampus and dentate gyrus in normal and reeler mice. J Comp Neurol 185:393–422.
Steward O, Falk PM (1986) Protein-synthetic machinery at postsynaptic sites during synaptogenesis: a quantitative study of the association between polyribosomes and developing synapses. J Neurosci 6:412–423.
Torres-Aleman I, Naftolin F, Robbins RJ (1990) Trophic effects of insulin-like growth factor-I on fetal rat hypothalamic cells in culture. Neuroscience 35:601–608.
Weibel ER (1979) Stereological methods, Vol 1, Practical methods for biological morphometry, pp 148–150. Orlando, FL: Academic.
Werther GA, Cheesman H, Russo V (1993) Olfactory bulb organ culture is supported by combined insulin-like growth factor-I and basic fibroblast growth factor. Brain Res 617:339–342.
Wimer RE, Wimer CC, Alameddine L (1988) On the development of strain and sex differences in granule cell number in the area dentata of house mice. Dev Brain Res 42:191–197.
Ye P, Carson J, D'Ercole AJ (1995) *In vivo* actions of insulin-like growth factor-I (IGF-I) on brain myelination: studies of IGF-I and IGF binding protein-1 (IGFBP-1) transgenic mice. J Neurosci 15:7344–7356.
Ye P, Xing Y, Dai Z, D'Ercole AJ (1996) *In vivo* actions of insulin-like growth factor-I (IGF-I) on cerebellum development in transgenic mice: evidence that IGF-I increases proliferation of granule cell progenitors. Dev Brain Res 95:44–54.
Zackenfels K, Oppenheim RW, Rohrer H (1995) Evidence for an important role of IGF-I and IGF-II for the early development of chick sympathetic neurons. Neuron 14:731–741.